STUDY OF NUCLEAR STATICS AND DYNAMICS USING THE WIGNER TRANSFORM*

S. SHLOMO
Department of Physics and Cyclotron Institute,
Texas A&M University,
College Station, Texas,
United States of America

I. Introduction

The Wigner phase-space distribution function[1], given as the shifted Fourier transform of the density matrix, provides a framework for an exact reformulation of non-relativistic quantum mechanics in terms of classical concepts. The Wigner distribution function (WDF), $f(\vec{r},\vec{p})$, is considered as a quantum mechanical generalization of the classical phase space distribution function. While basic observable, such as matter density and momentum density, are given by the same integrals over $f(\vec{r},\vec{p})$ as in classical physics, $f(\vec{r},\vec{p})$ differs from its classical analog by the fact that it can assume negative values in some regions. However, it is known that the WDF is a useful and convenient tool for the study of the static and the dynamical aspects of many-body quantum systems[2], and the equation of motion for $f(\vec{r},\vec{p})$ serves as a starting point for semi-classical approximations[3-6].

The aim of this talk is to present and discuss some recent results for static and dynamic properties of nuclei obtained by exact evaluation of the WDF. These results were obtained in collaboration with M. Prakash, J. P. Bondorf, B. S. Nilsson, F. E. Serr and V. M. Kolomietz.

II. The Wigner Distribution Function

Before presenting and discussing results obtained using the WDF let me first discuss properties and use of the WDF.

Given the wave function $\psi(\vec{r},t)$ one can construct the density matrix $\rho(\vec{r},\vec{r}',t) = \psi^*(\vec{r},t)\psi(\vec{r}',t)$. The corresponding Wigner transform (WT) is defined[1] as the shifted Fourier transform of $\rho(\vec{r},\vec{r}',t)$;

$$f(\vec{r},\vec{p},t)= \frac{1}{(2\pi)^3}\int d\vec{s}\; e^{i\vec{p}\cdot\vec{s}}\,\rho(\vec{r}+\frac{1}{2}\vec{s},\vec{r}-\frac{1}{2}\vec{s},t). \qquad (1)$$

*Supported in part by the National Science Foundation under contract #PHY-8109019.

The inverse transform is ($\hbar$=1),

$$\rho(\vec{r},\vec{r}',t)= \int d\vec{p}\; e^{-i\vec{p}\cdot(\vec{r}-\vec{r}')}\, f(\frac{\vec{r}+\vec{r}'}{2}\,,\,\vec{p},t). \qquad (2)$$

In the present work, we consider $\rho(\vec{r},\vec{r}',t)$ obtained assuming that the many-body wave function is a Slater determinant. In this case,

$$\rho(\vec{r},\vec{r}',t)= \sum_j n_j\, \psi_j^*(\vec{r},t)\psi_j(\vec{r}',t), \qquad (3)$$

where n_j are the occupation numbers, and $\psi_j(\vec{r},t)$ are the single-particle wave functions in the mean field.

Properties and Use of the WDF:

The WDF, $f(\vec{r},\vec{p},t)$, is a real function that may acquire negative values in certain regions of the phase space. The expectation value of an observable O is given by,

$$\langle\psi|O|\psi\rangle = \int d\vec{r}d\vec{p}\; f(\vec{r},\vec{p})\; O_W(\vec{r},\vec{p}), \qquad (4)$$

where $O_W(\vec{r},\vec{p})$ is the corresponding operator in Wigner space, in which r and p are numbers. In particular, we have for the matter, momentum and current densities;

$$\rho(\vec{r})= \psi^*(\vec{r})\psi(\vec{r}) = \int d\vec{p}\; f(\vec{r},\vec{p}) \qquad (5)$$

$$\tilde{\rho}(\vec{p})= \tilde{\psi}^*(\vec{p})\tilde{\psi}(\vec{p}) = \int d\vec{r}\; f(\vec{r},\vec{p}) \qquad (6)$$

$$\vec{J}(\vec{r}) = \int \frac{\vec{p}}{m}\, f(\vec{r},\vec{p})\; d\vec{p}. \qquad (7)$$

The integrals over f in (5) to (7) are the same as in the classical case. We thus consider f as the quantum-mechanical analog of the classical probability density in phase space. With this interpretation the WDF provides an intuitive alternative to the usual wave function formulation of the non-relativistic quantum mechanics. For example, considering the scaler product of wave functions, one finds[7] that

$$|\langle\psi_1|\psi_2\rangle|^2=(2\pi)^3 \int d\vec{r}\; d\vec{p}\; f_1(\vec{r},\vec{p})\; f_2(\vec{r},\vec{p}) \qquad (8)$$

where f_1 and f_2 are the WTs which correspond to ψ_1 and ψ_2, respectively. Also for $\psi(\vec{r})= \psi_1(\vec{r})\,\psi_2(\vec{r})$, one finds using (2) that

$$f(\vec{r},\vec{p}) = \int d\vec{p}'\; f_1(\vec{r},\vec{p}-\vec{p}')\; f_2(\vec{r},\vec{p}'). \qquad (9)$$

Note that the right hand sides (r.h.s.) of (8) and (9) have a simple interpretation in phase-space.

The equation of motion for $f(\vec{r},\vec{p},t)$ is derived directly from Schrödinger equation. For many-body problem a coupled hierarchy equations for reduced distribution functions can be derived by carrying Wigner transforms of the corresponding equations in terms of density matrices[4]. Kinetic equations for f are then obtained by truncating the set of equations. These kinetic equations (Vlasov, Boltzmann) are easy to derive though hard to justify. By taking *moments* $\int p^n dp$ of the kinetic equation one then derives hydrodynamic equations. Reaction cross sections can be derived by taking the limit $t\to\infty$ and integrating f over $\vec{r}$. For example, in the case of potential scattering, the probability for finding a particle with momentum $\vec{p}$ is given by[6]

$$\frac{dN}{d^3\vec{p}} = \lim_{t\to\infty} \int f(\vec{r},\vec{p},t)\, d\vec{r}. \qquad (10)$$

III. Applications

Some Features of the WDF: The function $f(\vec{r},\vec{p})$ has a complicated structure and is rarely studied. I'll first discuss some of its features in static and dynamical situations. The WTs which correspond to a plane wave and a Gaussian are:

$$\psi(\vec{r}) = \frac{1}{(2\pi)^{3/2}} e^{i\vec{k}\cdot\vec{r}}, \qquad f(\vec{r},\vec{p}) = \frac{1}{(2\pi)^3}\,\delta(\vec{p}-\vec{k}) \qquad (11)$$

$$\psi(\vec{r}) = \frac{1}{(4\pi)^{1/2}} \left(\frac{\nu}{\pi}\right)^{3/4} e^{-\nu r^2/2}, \qquad f(\vec{r},\vec{p}) = \frac{1}{\pi^3} e^{-(\nu r^2+p^2/\nu)}. \qquad (12)$$

It is seen from (11) that for a Fermi gas (FG), the WDF which corresponds to the one-body density matrix is given by

$$F(\vec{r},\vec{p}) = \frac{1}{(2\pi)^3}\,\Theta(p_F^2-p^2). \qquad (13)$$

An analytic expression for F can be derived for an N-dimensional harmonic oscillator (HO). The result is[8]

$$F_M^N(\varepsilon) = \frac{1}{\pi^N} e^{-\varepsilon} \sum_{K=0}^{M} (-1)^K L_K^{N-1}(2\varepsilon), \qquad (14)$$

where $L_n^\alpha(x)$ is the associated Laguerre polynomial, $\varepsilon=p^2+r^2$ with p and r are in units of $\sqrt{\hbar/\omega}$ and $1/\sqrt{\omega}$, respectively, and M is the highest major shell which is occupied (M=0,1, and 2 for ^{4}He, ^{16}O, and ^{40}Ca, respectively). In Fig. 1 are shown plots of (14) for 3-dimensional HO for several closed shell nuclei.

It is clearly seen that the WDF acquires negative values, in certain regions, which are much larger than the FG value. Fig. 2 shows $F_2^1(p,q)$ for 3 particles in the lowest states of one-dimensional (1D) HO potential well. For comparison, Fig. 3 shows the corresponding F for 3 particles in the lowest states of 1D infinite box of length a. It is quite interesting to see that the WDF of Fig. 3 exhibits considerably more structure than that of Fig. 2. This demonstrates the difficulty in the numerical evaluation of the WDF for large nuclei, using realistic 3D wave functions. Fig. 4 shows a cross-sectional cuts of the WDF, $f(z,k_z,r_\perp=k_\perp=0)$, obtained from time dependent Hartree-Fock (TDHF) wave functions for the head on $^{16}O+^{16}O$ collision at E/A=1.25 MeV (E_{lab}=80 MeV). The time $T=0.4\times10^{-21}$s has been chosen such that the two nuclei overlap considerably with each other. The figure shows that the dynamic WDF also has large negative values at certain regions.

Matter, Momentum and Energy Flow in Heavy-Ion Collisions:

Heavy-ion collision dynamics in deep inelastic and fusion reactions is characterized by a considerable rearrangement of the positions and momenta of several nucleons. In order to study the space-momentum correlation and obtain new insight into the dynamics of heavy-ion collisions we make use of the WDF. Rather than evolving the WDF itself, we construct it from wave functions resulting from a dynamical theory. For this we use the time dependent Hartree-Fock (TDHF) approximation. As an example, some results[2] for head-on collisions of $^{40}Ca+^{40}Ca$ at E/A=5.0 MeV (E_{Lab}=800 MeV) are presented in the following.

To investigate the flow of momentum during the reaction, we evaluate the quantity,

$$\tilde{f}(k_z,\vec{k}_\perp,t) = \int_{z\geq 0} f(\vec{r}_\perp,z,\vec{k}_\perp,k_z)\,d\vec{r}_\perp dz. \qquad (15)$$

In Fig. 5 we show a plot of this function for the $^{40}Ca + ^{40}Ca$ reaction of E/A = 5 MeV. Eq. (15) gives the momentum distribution in the positive halve of z space only. Therefore, at the lowest value of t we have a smooth distribution corresponding to the ground state momentum distribution of one nucleus centered around $k_z = (1/2)\,k_{rel}$. The plateau in the region $|\vec{k} - (1/2)\vec{k}_{rel}| \sim 0.6$ fm^{-1} is due to shell structure. During the interaction time, momentum components associated with nucleons transferred from the other nucleus, as well as components associated with collective excitations are present in the $z \geq 0$ space. These are clearly seen by the peaks and shoulders of the curves in Fig. 5. The distribution for the largest t still differs considerably from a totally thermalized distribution. The absence of two-body collisions in the TDHF approximation naturally leads to very slow thermalization of the separated fragments.

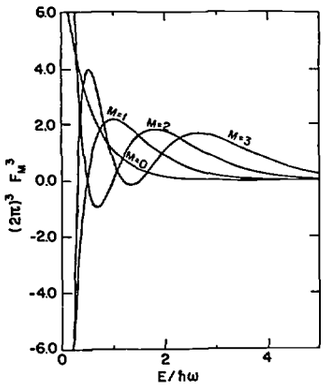

Fig. 1. The function $F_M^3(\varepsilon)$ as a function of the classical energy $E(=\varepsilon/2)$ for different values of M.

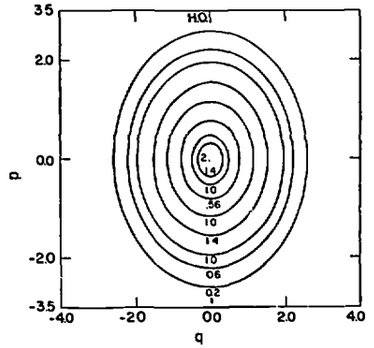

Fig. 2. The Wigner transform, $F_{\frac{1}{2}}^1(p,q)$, for 3 particles in the lowest states of a one-dimensional harmonic oscillator well. The contour values indicated in the figure are in units of $1/2\pi$. p and q are in units of $\sqrt{\hbar\nu}$ and $1/\sqrt{\nu}$, respectively, where ν is the size parameter of the well.

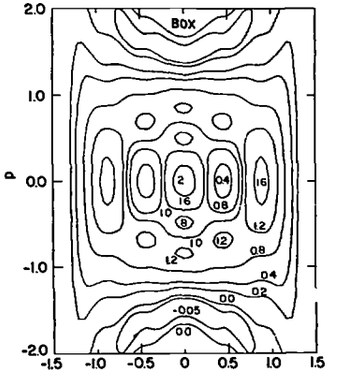

Fig. 3. The Wigner transform for 3 particles in the lowest states of a one-dimensional infinite box of length a. The boundary conditions are such that the wave functions vanish at, and outside the boundaries of the box. Contour values indicated in the figure are in units of $1/2\pi$ (note the symmetry of the plot). p and q are in units of K_F and π/K_F, respectively with $K_F = 3\pi/a$.

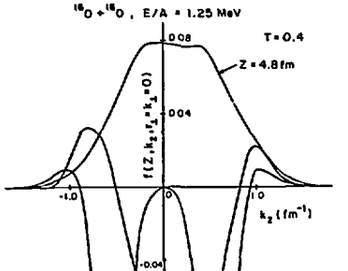

Fig. 4. Cross-sectional cuts of the WDF during the TDHF dynamics. Time is in units of 10^{-21} sec.

The flow of momentum and energy in the perpendicular direction might have important consequences on the dynamics. To quantify this aspect of heavy-ion collision dynamics, we investigate the behavior of the parallel and perpendicular components of the total kinetic energy during the reaction. In terms of the WDF, the kinetic energy density is defined by

$$\tau_W(\vec{r}) = \int (\hbar^2 k^2/2m)\, f(\vec{r},\vec{k})\, d\vec{k}, \qquad (16)$$

and the total kinetic energy T is given by

$$T = \int \tau_W(\vec{r})\, d\vec{r}. \qquad (17)$$

We separate the parallel and perpendicular components of T, denoted T_z and $T_\perp$, by replacing k^2 by k_z^2 or $k_\perp^2$ in Eq. (16). In Fig. 6 we show T_z, $T_\perp$ and T during the $^{40}Ca+^{40}Ca$ reaction at 5.0 MeV. At t = 0, $T_z = (1/2)T_\perp + T_{rel} - V_c$, where T_{rel} is the initial kinetic energy with which the ions are boosted towards each other, and V_c is the Coulomb interaction energy at the initial separation. As the two nuclei overlap, T_z, $T_\perp$ and T begin to oscillate. The change $T_\perp$ during the interaction time is comparable to that for T_z. These results imply that there is a considerable redistribution of energy between the ions during the reaction. In so far as the outcome of the TDHF dynamics is dependent on what happens during the interaction time, allowing dynamics to take place only in a plane and freezing the wave functions in the third direction could lead to significantly different results.

In diffusion models of nucleon transfers, quantitative predictions of the observables depend sensitively on the magnitude of the nucleon current from one ion to the other. We have carried out a microscopic dynamical calculation of the nucleon flow using the concept of a one-way current defined in terms of the WDF[9]. The one-way current density in the direction of a unit vector $\hat{z}$ is defined as,

$$j_+(\vec{r},t) = \int_{k_z \geq 0} (\hbar k_z/m)\, f(\vec{r},\vec{k},t)\, d\vec{k} \qquad (18)$$

Integrating (18) over the perpendicular components of space and momentum, the one-way current $\phi_+(z,t)$ across a plane at z is given by

$$\phi_+(z,t) = \int_0^\infty (\hbar k_z/m)\, \bar{f}(z,k_z,t)\, dk_z \qquad (19)$$

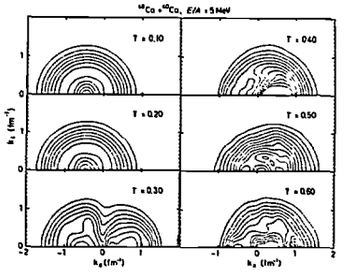

Fig. 5. The momentum distribution in the $z \geq 0$ space, as a function of the parallel and perpendicular components of momentum. Time is in units of 10^{-21} sec. Starting from the outermost one, the contours are associated with f = 1.0 (1.0) 12.0.

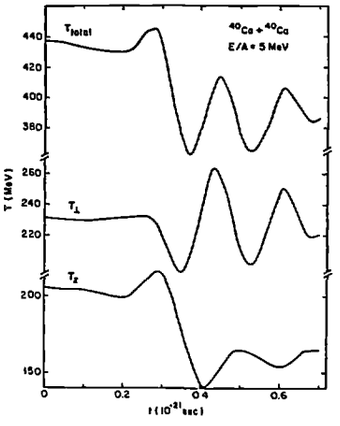

Fig. 6. The kinetic energy as a function of time. T_z and $T_\perp$ are the components of kinetic energy parallel and perpendicular to the reaction axis z($T = T_z + T_\perp$).

In Fig. 7 we show the one way current of particles $\Phi_0=\phi_+(z = 0,t)$, across the plane dividing the two ions, as a function of the fragment separation R(t). The coordinate R(t) is defined by

$$R(t) = (2/A) \int d^3\vec{r} \; |z| \; \rho(\vec{r},t) \qquad (20)$$

where A is the total number of particles, and $\rho(\vec{r},t)$ is the mass density.

We also show in Fig. 7 the results for the one way current Φ_0 obtained from two simplified models: the relative motion model and the tunnelling model.[9] In the relative motion model we move the frozen initial HF density profile of one of the ions past the z = 0 plane, with a time dependent average relative velocity determined from the TDHF calculations. The tunnelling model is based on the approach of Ko et al.[10] in which the one-way current is due to nucleons tunnelling through and over the potential barrier of the two ions. We use the potential obtained from the TDHF calculations to determine transmission probability. Comparing the combination of the one-way currents due to relative motion and tunnelling to the TDHF results, we find that, at distances large compared to the contact distance R_c, Φ_0^{TDHF} is almost entirely due to the relative motion. Near R_c, the sum of the contributions from relative motion and tunnelling is close to the calculated TDHF one-way current. The comparison is not as meaningful for very compact configurations because some of our approximations are no longer valid. Better agreement should be obtained by refining the models for the two contributions. Inside R_c and during the exit phase the ions are no longer spherical. Deformation should be taken into account in the integration over the facing surfaces of the two ions for the flux due to tunnelling and in the density and velocity dependence entering $\Phi_0^{rel\ motion}$. Also, Pauli blocking would reduce both contributions.

The Single Particle Response Function in Finite Nuclei:

Within the independent particle model, the response of the nucleus to the projectile scattering probe $\sigma(\vec{q},\vec{r})$ is defined by[11],

$$S(E,q) = \frac{1}{N} \sum_{i,f} \left|\langle\psi_f|\sigma|\psi_i\rangle\right|^2 \delta(E_f-E_i-E), \qquad (21)$$

where ψ_i and ψ_f are occupied and unoccupied states, respectively, and $N = \sum_i \langle\psi_i|\sigma^*\sigma|\psi_i\rangle$ is the normalization factor. The Pauli blocking factor is given by[12]

$$P(q) = \int dE \; S(E,q). \qquad (22)$$

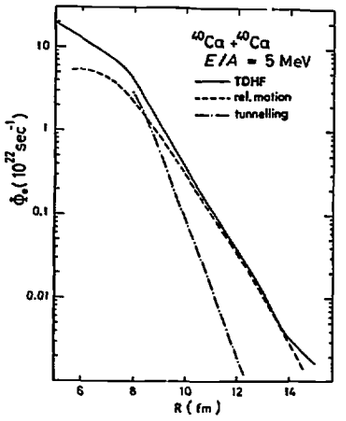

Fig. 7. The one-way currents as a function of the fragment separation R. The models are explained in the text.

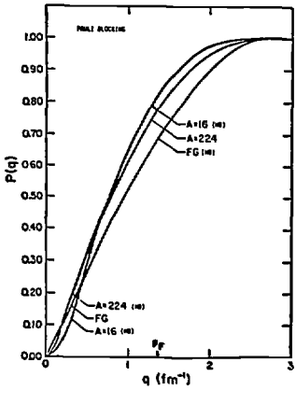

Fig. 8. The Pauli blocking factor for A = 16 ($\hbar\omega$ = 13.92 MeV) and A = 224 ($\hbar\omega$ = 6.73 MeV), compared with the Fermi-gas model P_F = 1.37 fm^{-1}.

Using (8) and (9), the matrix element in (21) can be written as[13],

$$\left|\langle\psi_f|\sigma|\psi_i\rangle\right|^2=(2\pi)^3\int d\vec{r}\ d\vec{p}\ d\vec{p}'\ f_\sigma(\vec{r},\vec{p}_i')\ f_f(\vec{r},\vec{p})\ f_i(\vec{r},\vec{p}+\vec{p}'), \quad (23)$$

where f_i, f_f and f_σ are the WTs of ψ_i, ψ_f and σ, respectively. The Pauli blocking factor is then given by,

$$P(q)=\frac{1}{N}\int d\vec{r}\ d\vec{p}\ d\vec{p}'\ f_\sigma(\vec{r},\vec{p}')\ F_a(\vec{r},\vec{p})\ [1-(2\pi)^3F_a(\vec{r},\vec{p}+\vec{p}')], \quad (24)$$

where $F_a=\sum f_i$ is the WT on the a-nucleon system. Note that (23) and (24) are of the form that one may write down under the assumption that f is a probability density in phase space.

In the Born approximation, $\sigma = e^{i\vec{q}\cdot\vec{r}}$ and $f_\sigma(\vec{r},\vec{p})=\delta(\vec{p}'-\vec{q})$. In this case (23) and (24) can be reduced to 6D integrals. For the FG, one recovers the widely used Lindhards function[14] from (23). Using (13) in (24) one finds the well-known results,

$$P(q) = \begin{cases} \frac{3}{4}x\,(1-x^2/12) & x\le 2 \\ 1 & x\ge 2 \end{cases}, \quad (25)$$

where $x = q/p_F$ and p_F is the Fermi momentum. Using the HO model for ψ, eq. (23) can be evaluated to give[13],

$$S(E,q)=\frac{1}{a}\sum_{k=1}^{\infty}\delta(k\hbar\omega-E)(q^2/2)^k\,e^{-q^2/2}$$
$$*\left[\sum_{n=0}^{M}\frac{n!}{(n+k)!}\,L_{M-n}^{5/2}(0)\,L_n^{-1/2}(0)\,L_{2n}^{2k}(q^2)\right. \quad (26)$$
$$\left.-\sum_{n=0}^{M-k}\frac{n!}{(n+k)!}\,L_{M-k-n}^{5/2}(0)\,L_n^{-1/2}(0)\,L_{2n}^{2k}(q^2)\right],$$

where $a = L_M^3(0) = \binom{M+3}{3}$ and q is in units of $\hbar\sqrt{\nu}$. A simple expression can be also derived for P(q). It is seen from Fig. 8 that the HO values for P(q) are quite similar to the FG values, in disagreement with experiment[12]. This calls for a better approximation for $\sigma(\vec{q},\vec{r})$.

In summary, I have presented some results concerning nuclear statics and dynamics obtained with the help of the WDF. While in principle it provides no more information than obtained from wave functions, the WDF sometimes provides a convenient way of calculating quantities that have a classical or semi-classical analog. Therefore, the WDF is a useful function to utilize in the study of many-body system.

References

[1] E. P. Wigner, Phys. Rev. 40, (1932) 749.

[2] M. Prakash, S. Shlomo, B. S. Nilsson, J. P. Bondorf and F. E. Serr, Nucl. Phys. A385, (1982) 483; and references therein.

[3] N. L. Balazs and G. G. Zipfel, Jr., Ann. of Phys. 77, (1973) 139.

[4] G. F. Bertsch, Many-Body Dynamics of Heavy Ion Collisions, in Les Houches Lecture Notes, ed. R. Ballian (North-Holland, Amsterdam 1978) pp. 178-262.

[5] P. Ring and P. Schuck, The Many-body Problem (Springer, New York, 1980) Ch. 13, and references therein.

[6] P. Carruthers and F. Zachariasen, Preprint CALT-68-856, 1982, and references therein.

[7] R. F. O'Connell and E. P. Wigner, Phys. Lett. 85A, (1981) 121.

[8] S. Shlomo and M. Prakash, Nucl. Phys. A357, (1981) 157.

[9] M. Prakash, S. Shlomo, B. S. Nilsson, J. P. Bondorf and F. E. Serr, Phys. Rev. Lett. 47, (1981) 898.

[10] C. M. Ko, G. F. Bertsch and D. Cha, Phys. Lett. 77B, (1978) 174.

[11] A. L. Fetter and J. D. Walecka, Quantum Theory of Many-Particle Systems (McGraw-Hill, N. Y., 1971).

[12] G. F. Bertsch and O. Scholten, Phys. Rev. C25, (1982) 804.

[13] S. Shlomo, Phys. Lett. in print.

[14] J. Lindhard, K. Van Videnak, Selsk. Mat. Fys. Medd. 28, (1954) No. 8.